Development of a high stability L-band radiometer for ocean salinity measurements

William J. Wilson, Alan Tanner
Jet Propulsion Laboratory, California Institute of Technology
Pasadena, CA 91109

Fernando Pellerano
Goddard Space Flight Center
Greenbelt, MD 20771

Abstract- Future sea surface salinity missions will require L-band radiometers to have calibration stabilities of ≤ 0.05 K over 2 days. This research program has focused on determining the optimum radiometer requirements and configuration to achieve this objective. System configuration and component performance have been evaluated with radiometer test beds at both JPL and GSFC. The GSFC testbed uses a cryogenic chamber that allows long-term characterization at radiometric temperatures in the range of 70 - 120 K. The research has addressed areas including component characterization as a function of temperature, system linearity, optimum noise diode injection calibration and precision temperature control of components.

I. Introduction

Aquarius is a new NASA Earth System Science Pathfinder (ESSP) mission to measure global sea surface salinity (SSS). Salinity data will permit estimates of sea surface density, or buoyancy, which drives the ocean's three-dimensional circulation. In the tropics, Aquarius data will facilitate the understanding of surface buoyancy on important air-sea interaction processes that affect climate changes. Surface salinity will also provide a strong constraint on the surface water budget over 70% of the Earth's surface. The baseline science data product from the Aquarius mission will be a monthly global surface salinity map with 100-km spatial resolution and with an accuracy of 0.2 practical salinity units over the 3-year mission life. (The practical salinity unit (psu) approximately corresponds to parts per thousand of salinity.)

.

The calibration stability requirement for the Aquarius radiometers is 0.15 K over two days. Future SSS missions will require SSS measurements with an accuracy of 0.1 psu and with a smaller spatial resolution. This will require the L-band radiometers to have calibration stabilities of ≤ 0.05 K over 2 days. Note that this is a factor of 3 improvement over the Aquarius radiometer requirement. The main focus of this Instrument Incubator Program (IIP) research is to determine the optimum radiometer requirements and configuration to achieve the ≤ 0.05 K calibration stability.

II. Radiometer Component Tests

Radiometer test beds have been assembled at both the Jet Propulsion Laboratory (JPL) and the Goddard Space Flight Center (GSFC) to test radiometer components with regard to their temperature stability characteristics. A block diagram of the JPL testbed is shown in Fig. 1. Slow temperature sweeps of the device under test (DUT) were made while rest of radiometer was held at a constant temperature. The components tested included SMA cables, directional couplers, ferrite isolators, FET switches, PIN diode switches, and a frequency diplexer. In some of these components, the loss was higher than expected and in a few cases, a hysteresis in the loss characteristics was observed.

The GSFC radiometer testbed was built with a cryogenic load and operated in a thermal vacuum chamber, as shown in the block diagram in Fig. 2. A model for the input cable losses, based its temperature distribution was developed which included the connector losses and mismatches. A sensitivity analysis to these parameters suggested that the input temperature to the radiometer was stable with an uncertainty of ~0.03 K RSS, which is adequate for the subsequent testing.

III. Radiometer Calibration Technique

Another area in this research was the development of a calibration technique to provide the required calibration stability, while obtaining the lowest NEDT performance. We have measured the gain and receiver noise temperature spectra and apply these data to a new calibration scheme which achieves optimum NEDT performance by applying long running averages of the receiver noise temperature and of the receiver gain to the brightness.

Figure 3 illustrates the topology of a Dicke radiometer with noise injection, along with an example of the radiometer's output voltage versus time to illustrate the basic measurement sequence. The calibration circuits of this radiometer consist of the Dick switch and noise diode. The Dicke switch alternates between the antenna and the reference load temperatures, T_A and T_o, and the noise diode adds a calibrated antenna-equivalent noise temperature, T_{ND}, to the received signal. As shown, the reference load and noise diodes are applied every τ seconds with duty cycles d_o and d_N, respectively, leaving a remainder of $1-d_o-d_N$ duty cycle to measure the antenna noise temperature. The noise diode is injected after the Dicke switch in Figure 1, so the noise diode response can be measured in either mode of the Dicke switch.

For our calculations, however, we will assume that the noise diode is injected only while this switch is in the reference mode. The response of the radiometer to each source is integrated and recorded separately as C_o, C_N, and C_A, and all measurements are subject to the unknown and time variable quantities of receiver gain, G, and additive receiver noise temperature, T_r, as summarized in the figure. In the simplest mode of operation the antenna temperature T_A can be estimated from each measurement cycle as

$$T_A = T_o - (C_o - C_A)\frac{T_{ND}}{C_{ND}} \qquad (1)$$

where we see that G and T_r from the expressions of Figure 1 cancel. Equation (1) is inefficient from a noise standpoint however, since it makes no assumptions about the stability of the receiver gain or the receiver noise temperature other than that these factors are common to all of the measurements within the interval τ. If, on the other hand, we know that G or T_r are stable over longer time scales we can reformulate the calibration as follows: we estimate the antenna brightness temperature according to

$$\mathbf{T_A = G^{-1}C_A - T_r} \qquad (2)$$

where

G^{-1} = the inverse of gain

C_A = a boxcar integration of the antenna response lasting τ_A seconds. This interval (τ_A) is set by mission requirements (τ_A=12 seconds for Aquarius) and may be greater than τ (the Dicke interval).

τ_g = gain estimation integration time

τ_r = receiver noise estimation integration time

d_o = reference load duty cycle

d_N noise diode duty cycle

The measurements of G^{-1} and T_r are computed from running averages spanning τ_g and τ_r seconds, respectively, as shown in Figure 3, according to

$$G^{-1} = \left(d_o \frac{T_o + T_r}{C_o} + d_n \frac{T_o + T_{ND} + T_r}{C_N} \right) \frac{1}{d_o + d_N} \qquad (3)$$

and

$$T_r = C_o \frac{T_{ND}}{C_N - C_O} - T_o \quad . \qquad (4)$$

The following models for the gain and receiver noise spectra were used:

$$\mathbf{S(G) = a_g + \frac{b_g}{f}}, \text{ and } \mathbf{S(T_r) = a_r + \frac{b_r}{f}},$$

where a = white noise which depends on B, τ, d and b is fit to system measurements. The system parameters and the optimization results are shown in Table 1.

System parameters:				**τ_A=12 s** **b_r=6.5x10^{-6} K^2/Hz** **b_g=2.0x10^{-9} /Hz** **T_r=255 K** **T_o=295 K** **T_{ND}=500 K** **T_A=100 K** **B=20 MHz**		
τ_r (s)	τ_g (s)	d_o	d_N	**NEDT (K)**	$/\Delta T_{TP}^*$
157812	96	**0.13**	**0.13**	0.038	1.64
5000	86	0.19	0.10	0.038	1.66
5000	89	**0.14**	**0.14**	0.038	1.67
1000	71	0.23	0.12	0.040	1.75
1000	69	**0.18**	**0.18**	0.040	1.76

notes: **highlighted** indicates constrained parameter

Table 1. Results from the optimization

These results show that an NEDT within a factor of 1.7 of a total power radiometer can be achieved with this observing technique. Additional details for this technique are found in Tanner [1].

III. Radiometer Linearity

A 'constant deflection' method was used to test and characterize the radiometer linearity. Using this approach, nonlinearities are observed as deviations of the noise diode deflection as the antenna noise temperature changes. This method offers the advantage that it can be applied to the complete radiometer system, as opposed to just the final detector circuit. In fact, this method can often be applied without any special accommodations or tests since the routine data from any noise adding radiometer may be sufficient to characterize the linearity of the system.

Fig. 4 shows the laboratory configuration of the deflection test. The antenna in this case was replaced with a cold source and an injected noise source which combined could be adjusted between ~30K and 4700K, well above and below the expected operational range. Also, the noise diode was injected after the Dicke switch so that the deflection can be measured in both the 'antenna' and 'reference' modes of the switch. With both of these measurements we can normalize the antenna deflections and examine the linearity with the deflection ratio

$$D = \frac{V_{AN} - V_A}{V_{ON} - V_O} \qquad (5)$$

where the four voltages represent the response to the antenna, antenna plus noise diode, ambient temperature reference, and reference plus noise diode. In a linear system with no mismatches- D should always be unity. If the system is not linear then D will change as the antenna noise temperature changes.

Fig. 5 shows the results of this linearity test. The system has a gain expansion behavior, as expected from the detectors, and gain compression at the higher levels. The response can be linearized very successfully with an error < 0.04%, using a third order polynomial fit. These results also showed a "bias" in the deflection ratio due to the impedance mismatch of the Dicke switch between the antenna and load ports. This effect shows up due to the coupler's imperfect isolation. Placing an isolator between the Dicke switch and the coupler eliminated this problem.

,

ACKNOWLEDGMENT

This work represents one phase of research carried out at the Jet Propulsion Laboratory, California Institute of Technology, under contract with the National Aeronautic Space Administration.

REFERENCES

[1] Tanner, A., Wilson, W., Pellarino, F., "Development of a High Stability L-band Radiometer for Ocean Salinity Measurements", Proceedings of the 2003 International Geoscience and Remote Sensing Symposium , July21-25, 2003, Toulouse, France.

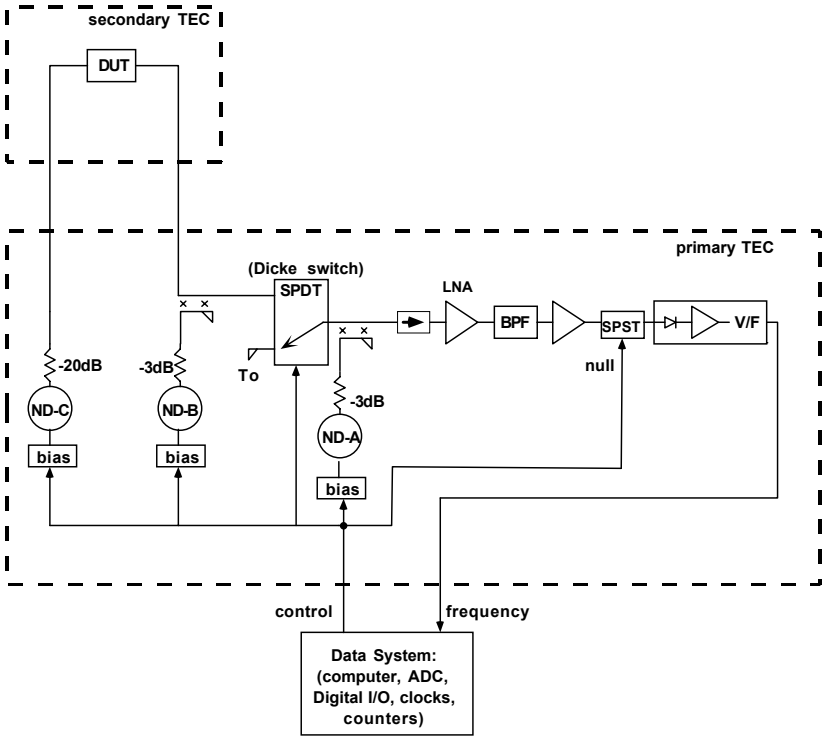

Fig. 1. Block diagram of JPL testbed showing Device Under Test (DUT)

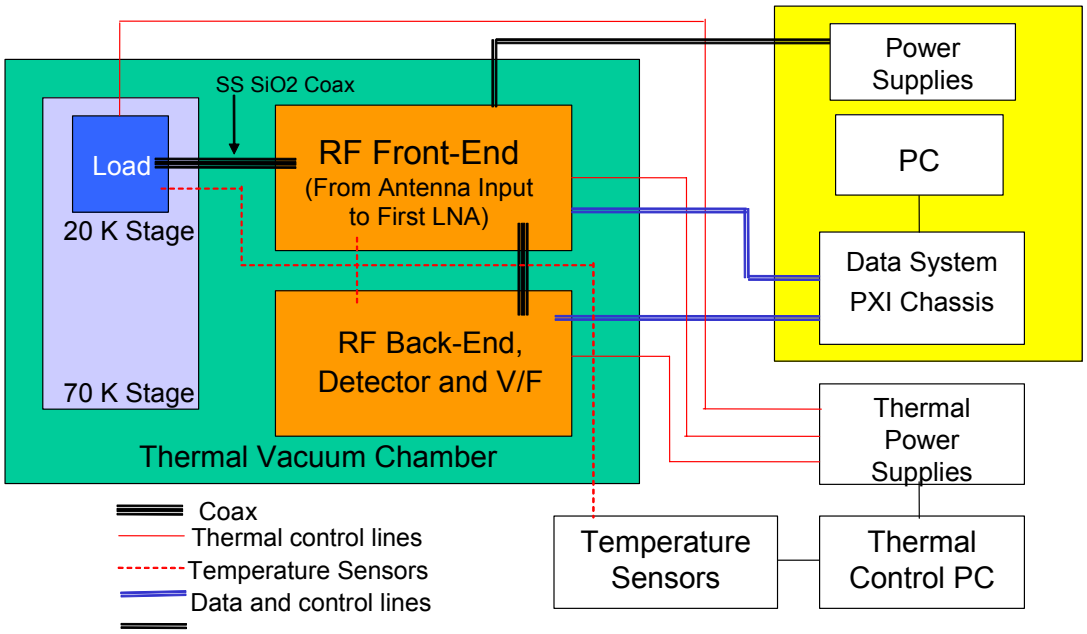

Fig. 2. Block diagram of GSFC cryogenic radiometer testbed

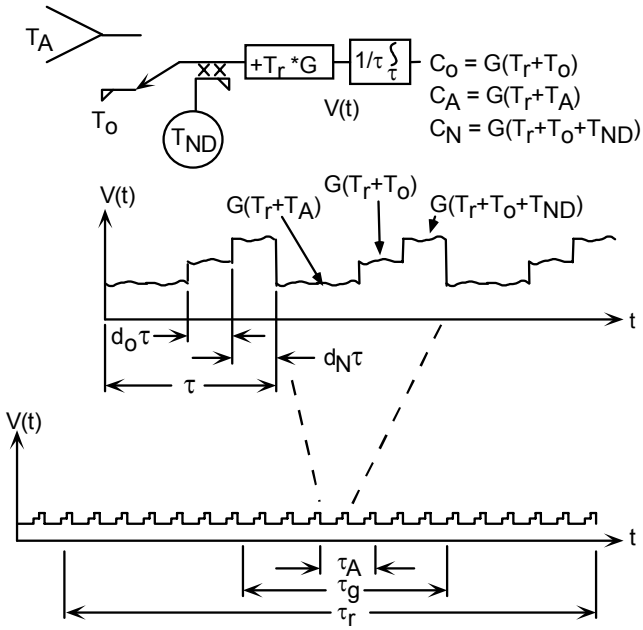

Fig. 3. Radiometer and timing model for NEDT optimization

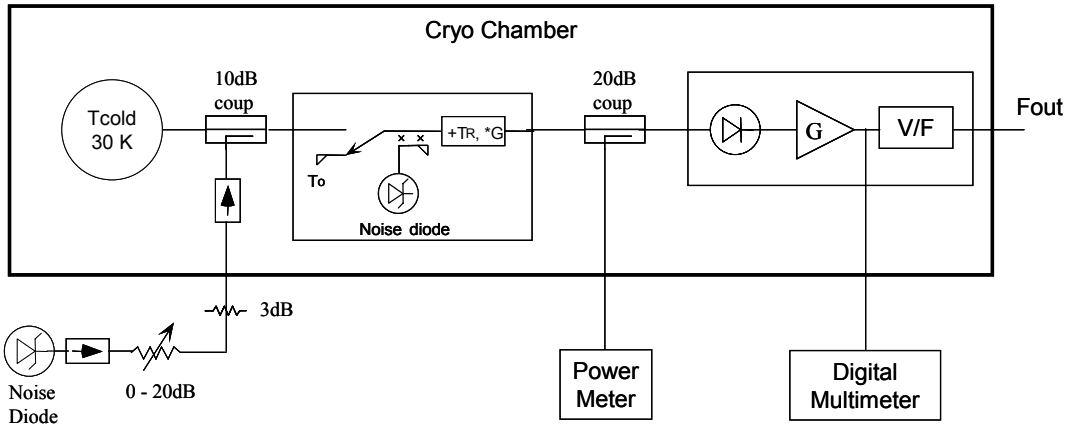

Fig. 4. Laboratory setup for radiometer linearity tests

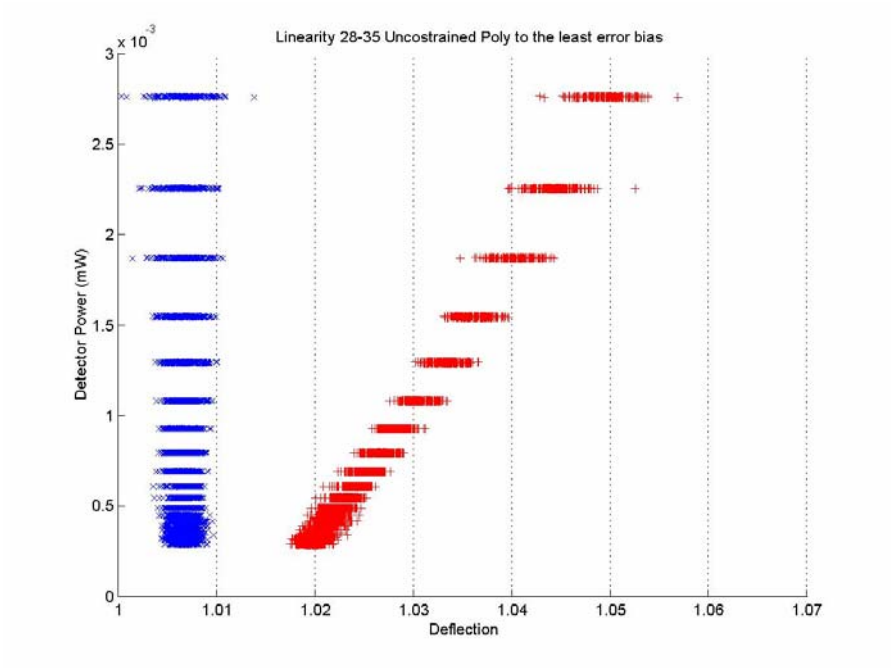

Fig. 5. Corrected and uncorrected radiometer deflections